Numerical Analysis of Anisotropic Influence of Mode-I Fracture Toughness under Dynamic Loading for Rock using GPGPU-based Three-Dimensional Combined Finite-Discrete Element Method (FDEM)

IOP Conf. Series: Earth and Environmental Science **861** (2021) 032077 doi:10.1088/1755-1315/861/3/032077

Numerical Analysis of Anisotropic Influence of Mode-I Fracture Toughness under Dynamic Loading for Rock using GPGPU-based Three-Dimensional Combined Finite-Discrete Element Method (FDEM)

G.J. Min[1], D. Fukuda[3], S.W. Oh[4], Y. Nara[5], H. Liu[6], S.H. Cho[1,2]

[1]Department of Mineral Resources & Energy Engineering, Jeonbuk National University, Jeollabuk-do, 561-756, South Korea
[2]Department of Energy Storage & Conversion Engineering of Graduate School, Jeonbuk National University, Jeollabuk-do, 561-756, South Korea
[3]Faculty of Engineering, Hokkaido University, Hokkaido 060-8628, Japan
[4]Deep Subsurface Research Center, Geological Environment Division, Korea Institute of Geoscience and Mineral Resources, 124, Gwahak-ro Yuseong-gu, Daejeon, 34132, Korea
[5]Graduate School of Engineering, Kyoto University, Kyoto 615-8540, Japan
[6]School of Engineering, College of Sciences and Engineering, University of Tasmania, Hobart, Tasmania 7001, Australia

The corresponding author's e-mail address: chosh@jbnu.ac.kr

Abstract. The anisotropic characteristics of rock are responsible for diverse and difficult-to-predict crack propagation and fracturing behaviors that manifest under various loading-rate conditions. In granitic rock, anisotropy makes predicting Mode I fracture toughness under different loading-rate conditions across all three orthogonal planes difficult. The reality compounds this difficulty that anisotropy is extremely difficult to quantify experimentally, and it has proven challenging to model this fracturing process (i.e., crack initiation and propagation) and its associated stress distribution. Accordingly, no in-depth model of the underlying fracture process for anisotropic rocks under quasi-static and dynamic loading conditions exists to date. An accurate simulation capable of describing the fracture process is necessary to close this gap. We successfully simulated the dynamic fracture process using a Finite-Discrete Element Method (FDEM) along with the New Self-Consistent Scheme. A Mode I fracture toughness test for an SNDB granite specimen under quasi-static and dynamic loading conditions was simulated using a GPGPU-based 3D combined FDEM and compared Mode I fracture toughness and behavior. We discuss the effect of anisotropic characteristics and loading-rate dependency on crack propagation.

1. Introduction

Rocks exhibit mechanical anisotropy due to its origin. Granitic rock is frequently studied [1-5] for its high engineering values. Granite is known to have frangible planes which are orthogonal to each other. The most fragile of these is known as the Rift-plane, the second most fragile plane (perpendicular to the Rift-plane) is referred to as the Grain-plane, while the plane perpendicular to both of these is the Hardway-plane. Several researchers have reported how anisotropy, perhaps the result of pre-existing microcracks induced by long-term geological loadings, might result in varied crack propagation and fracturing under diverse load conditions. Orthotropy, for example, affects the granite's tensile strength [2], fracture toughness [3, 5, 6], and elasticity [7]. There is, however, no detailed understanding of the mechanism by which fractures propagate in anisotropic rocks under quasi-static and dynamic loading conditions, as it has proven extremely difficult to quantify anisotropy and capture this fracturing process experimentally (i.e., crack initiation and propagation) and associated stress distribution. An accurate simulation that recreates the fracture process will improve our understanding of this process. The combined Finite-Discrete Element Method (FDEM) initially proposed by Munjiza [8] has gained traction and today is used in various engineering simulations. The FDEM combines the advantages of using both finite and discrete elements, enabling modeling of stress wave propagation throughout the intact rock, crack initiation and propagation, and interaction between discrete elements. We recently developed a state-of-the-art 3D combined finite-discrete element code, which we applied in this study using a General-purpose graphics processing unit (GPGPU). In this study, we used a new self-consistent scheme (NSCS) [9] to model the orthotropic elasticity of granite with pre-existing microcracks. We assumed that penny-shaped microcracks were randomly distributed (i.e., a plane perpendicular to Grain-axis) within the intact elastic granite body. The mutually orthogonal micro-cracks (i.e., planes perpendicular to Rift-axis and Hardway-axis) were also inserted. This process incorporated experimentally acquired P-wave velocity data for each orthogonal direction of a granite specimen. The effective elasticity tensor for the granite was computed after penny-shaped microcracks were inserted into an intact elastic body. The combined FDEM was then used to reproduce the Mode I fracture toughness test for a Straight Notched Disc Bend (SNDB) granite specimen under quasi-static and dynamic loading conditions. In the final section of this paper, we discuss the effects of anisotropic characteristics on crack propagation under different loading-rate conditions.

2. Modeling of anisotropy of granite using the NSCS

To model the orthotropy of granite, the New Self-Consistent Scheme (NSCS) was applied. The NSCS models the anisotropic elasticity of rock, accounting for the distribution of pre-existing microcracks. In modeling this, we assumed that the penny-shaped microcracks were randomly distributed along a plane perpendicular to Grain-axis at an intact elastic body. Mutually orthogonal micro-cracks (i.e., along planes perpendicular to the Rift-axis and the Hardway-axis) were also inserted. (see Fig. 1)

The effective elastic tensor was determined to apply orthotropy of rock in the numerical simulation. The effective elastic tensor, C^*_{ijkl}, was calculated using the measured values of elastic wave velocity in granite, as determined using the NSCS process. First, elastic wave velocities were inputted as parameters. Whenever microcracks for each orthogonal plane are inserted in rock, the effective elastic tensor, and the theoretical elastic velocity at this time are updated. Rock was initially an intact elastic body, and its elastic modulus and poison's ratio were assumed to be 80 GPa and 0.25 [9], respectively. Then, the theoretical elastic velocity was compared with the measured elastic wave velocity, and the effective elastic tensor is updated iteratively until the error between the theoretical and measured elastic velocity is minimal. The theoretically calculated values of the effective elastic constants are summarized in Table 1. The average density of the granite was $2600\,kg/m^3$. The values of the measured elastic wave velocities ($P^{measured}_{hardway} = 4870m/s$, $P^{measured}_{grain} = 4700m/s$, $P^{measured}_{rift} = 4120m/s$) are within 5% of the theoretical elastic wave velocities. ($P^{calculated}_{hardway} = 4970m/s$, $P^{calculated}_{grain} = 4710m/s$, $P^{calculated}_{rift} = 4590m/s$)

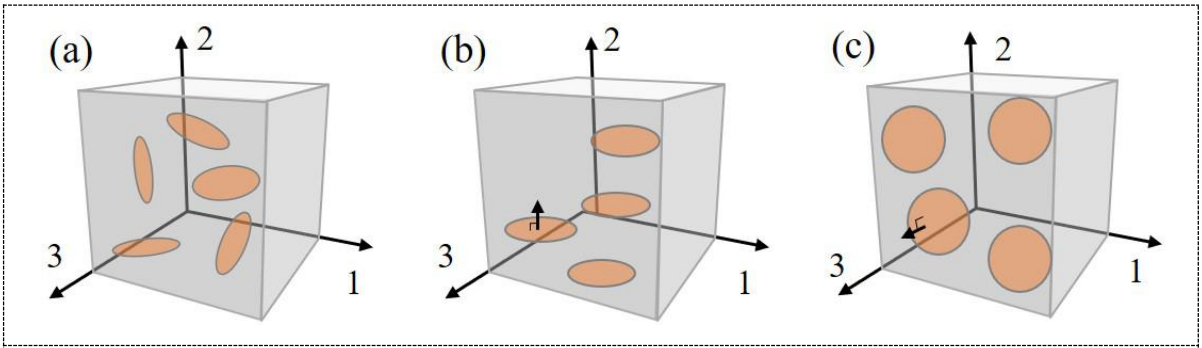

Figure 1**.** The microscopic crack distribution model (a) type 0; randomly positioned micro-cracks, (b) type 2; micro-cracks vertical to axis-2, and (c) type 3; micro-cracks vertical to axis-3.

Table 1. Effective elastic tensor for granite

Effective elastic tensor, $\boldsymbol{C^*_{ijkl}}$ (GPa)											
C^*_{1111}	C^*_{1112}	C^*_{1113}	C^*_{1122}	C^*_{1123}	C^*_{1133}	61	12	9.3	0	0	0
C^*_{1112}	C^*_{1212}	C^*_{1213}	C^*_{1222}	C^*_{1223}	C^*_{1233}	12	56	8.7	0	0	0
C^*_{1113}	C^*_{1213}	C^*_{1313}	C^*_{1322}	C^*_{1323}	C^*_{1333}	9.3	8.7	40	0	0	0
C^*_{1122}	C^*_{1222}	C^*_{1322}	C^*_{2222}	C^*_{2223}	C^*_{2233}	0	0	0	19	0	0
C^*_{1123}	C^*_{1223}	C^*_{1323}	C^*_{2223}	C^*_{2233}	C^*_{2333}	0	0	0	0	19	0
C^*_{1133}	C^*_{1233}	C^*_{1333}	C^*_{2233}	C^*_{2333}	C^*_{3333}	0	0	0	0	0	23

3. Numerical modeling of dynamic SNDB test

To analyse the effect of anisotropy on rock fracture process, the dynamic SNDB test for granite was reproduced by GPGPU based FDEM. In this section, a brief review of the dynamic SNDB test combined with split Hopkinson pressure bar (SHPB) is firstly reviewed. After that, the numerical analysis was performed for the dynamic SNDB test to investigate the fracture behavior of anisotropic rock.

3.1. Review of dynamic SNDB test combined with SHPB

The Straight Notched Disc Bend (SNDB) method has been used to determine the Mode-I fracture toughness of rock materials due to several advantages, such as the ease of specimen preparation, good applicability to the apparatus (e.g., SHPB, Hoek cell, etc.). Several researchers [4-6,13] have been performed the Mode-I fracture toughness test for rock specimens based on the SNDB method under quasi-static and dynamic loadings to evaluate the Mode-I fracture toughness and examine the crack propagation behavior. In this section, the dynamic SNDB test combined with SHPB is briefly introduced. A detailed description of the dynamic SNDB test can be found elsewhere [5]. To apply the SNDB method in the dynamic test, an SNDB specimen is applied (see Fig. 2(a)) and has its Mode I dynamic fracture toughness K^D_{IC} calculated using the following equation:

$$K^D_{IC,SNDB} = Y_{I,SNDB}\ \frac{P_{cr}}{4Rt}\sqrt{\pi a} \tag{1}$$

where a is the initial notch length, R is the specimen radius, t is sample thickness, P_{cr} is the maximum compressive force applied to the SNDB at failure, and $Y_{I,SNDB}$ is a dimensionless stress intensity factor. $Y_{I,SNDB}$ is expressed by $Y_{I,SNDB} = m(S/R) + n$ with m and n dependent on the t/R and a/t ratios. The values of m and n are determined by line fitting. In this study, the value of a was 4 mm, R was

18.5 mm, and t was 20 mm. Accordingly, the estimated values of m and n were 5.9 and 0.42, respectively, which resulted in $Y_{I,SNDB} = 3.4$. The opening of the notch was 1 mm.

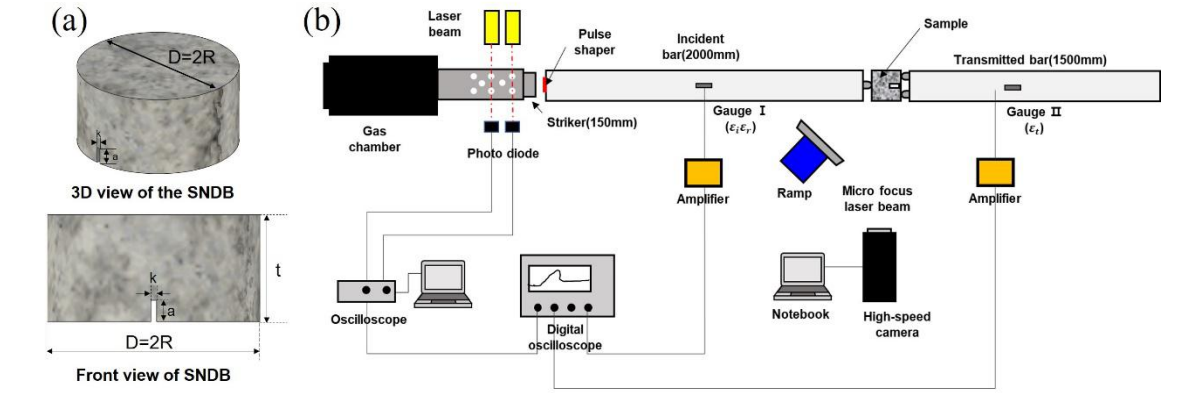

Figure 2. Schematic diagrams of (a) test specimen and (b) SHPB system for the dynamic SNDB test

The SHPB system was used to load the SNDB sample dynamically. Fig.2(b) illustrates the SHPB system, which consists of a striker bar, an incident bar, a transmitted bar, and a data acquisition system. Two semi−conductor strain gauges are mounted, one at the center of the incident bar and one at the center of the transmitted bar. Our SNDB sample was sandwiched by specially manufactured jigs attached to the incident and transmitted bars. The striker bar is shot with the gas gun, and as the striker bar collided with the end of the incident bar, a one-dimensional elastic stress wave propagated towards the SNDB specimen. The pulse shaping technique was applied to achieve the dynamic stress equilibrium of the test sample. Some of the stress waves are reflected at where the incident bar met the rock sample, while the remaining portion was transmitted into the rock. The transmitted stress wave propagated within the rock towards the transmitted bar. The stress wave is reflected and retransmitted once it hit the interface of the rock and the transmitted bar.

The SNDB rock sample is subjected to dynamic 3-point bending, resulting in the rock being split into two halves. The time history of strain in the transmitted bar, with Young's modulus and the cross-sectional areas of the transmitted bar, was used to calculate the applied load (P) using. P_{cr} was thus computed as the maximum value of P while dynamic fracture toughness it was using Eq. (1). The strain gauge mounted on the incident bar and transmitted bar measured the incident pulse (ε_i), reflected pulse (ε_r), and transmitted pulse (ε_t). Assuming a homogeneous deformation of the specimen, one-dimensional elastic wave propagation theory suggests that the forces at both ends of the sample can be calculated using Eqs. (2) ~ (4):

$$P_1(t) = EA[\varepsilon_i(t) + \varepsilon_r(t)] \quad (2)$$

$$P_2(t) = EA\varepsilon_t(t) \quad (3)$$

$$P_{Average}(t) = (P_1(t) + P_2(t))/2 = EA/2[\varepsilon_i(t) + \varepsilon_r(t) + \varepsilon_t(t)] \quad (4)$$

where A is the cross-section area, E is the elastic modulus of the bar, and $P_{Average}(t)$ is the average specimen load.

3.2. Numerical modeling of dynamic SNDB test

The numerical simulation model for the GPGPU based FDEM of SNDB granite sample subjected to quasi-static and dynamic loading by SHPB. To simulate the dynamic SNDB test, an SHPB system using an SNDB specimen was designed, as shown in Fig. 3(a). The SHPB system includes an incident bar (diameter: 38mm, length: 2m) and transmitted bar (diameter: 38mm, length: 1.5m). The rock specimen was placed between the incident bar and the transmitted bar. An elastic stress wave profile

was then entered as a dynamic load at the end of the incident bar, which was measured from the dynamic SNDB experimental test (see Fig. 2(a)).
The quasi-static model was also generated to compare the fracture behavior with the dynamic SNDB test (see Fig. 3(b)). A loading rod was placed in the top and bottom of the SNDB specimen; the top-loading rod applied loading to the specimen with constant velocity, while the bottom rod was fixed. The loading velocity was set at 1mm/s to satisfy the quasi-static condition in the specimen.
All models are discretized as tetrahedral elements (TET4), and the cohesive elements (CE6) are inserted to all TET4 boundaries only in the rock specimen. Because the potential crack pathways fell only along the boundaries between the TET4 element in the GPGPU based FDEM, a fine mesh are required for realistic crack propagation, necessitating a significant amount of calculation. Therefore, to boost up the calculation speed, a single NVIDIA Titan V GPGPU accelerator was utilized.
The input parameters used in the GPGPU based FDEM (Table 2) are based on the physical and mechanical properties of granite [10] as experimentally determined. The rock specimen was also modeled as an orthotropic elastic body, where the effective elasticity constant are inputted, as shown in Table 1. To determine the effect of orthotropy on crack propagation, the fracture plane was placed in different orthotropic planes. When a different orthotropic fracture plane should be considered, the constant value in the effective elasticity tensor was aligned with an orthogonal anisotropy plane corresponding to the desired fracture plane.

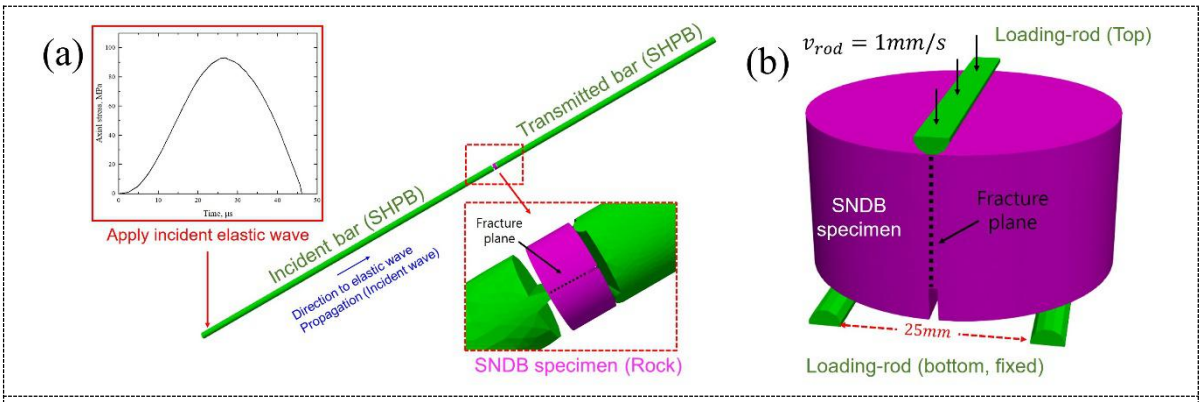

Figure 3. Numerical simulation model for (a) dynamic and (b) quasi-static SNDB test

Table 2. GPGPU based FDEM input parameters for simulated SNDB test

Parameter	Unit	Granite	Steel
Density (ρ)	kg/m^3	2600	7850
Young's modulus (E)	GPa	42	200
Poisson's ratio (v)	-	0.22	0.25
Microscopic tensile strength (T_s)	MPa	5	-
Microscopic cohesion (c)	MPa	25	-
Microscopic internal friction angle (ϕ)	Degrees	60	-
Microscopic Mode I fracture energy (G_{If})	N/m	60	-
Microscopic Mode II fracture energy (G_{IIf})	N/m	120	-

Artificial cohesive penalty (P_{open}, P_{tan},$P_{overlap}$)	GPa	$10E_{rock}$	$10E_{steel}$

3.3. Numerical simulation result

Significant differences in the fracture process between the quasi-static and dynamic loading states were detected, as shown in Fig.4. Figs. 4(a) and Figs. 4(b) presents the distribution of maximum principal stress (PS1) and macro-crack (open-crack). In both Figures, stress concentration is present at the crack tip. Note that, in the PS1, the negative value is compression while the positive value is tensile stress. Based on these figures, tensile stress in the crack tip is significant for crack initiation and propagation. Fig. 4(a) shows the stress distribution and fracture processes, which corresponds to the quasi-static loading rate model (within 15 ms ~ 29 ms). The crack is initiated at the front of the specimen notch tip at 15ms. At 18 ms, the crack begin to propagate along the loading direction. At 21 ms, the crack, which is almost flat, continuously propagates in the loading direction. At 29 ms, the tensile stress is continuously concentrated at the crack tip and propagated along the loading direction, and completely split into two fragments. Fig. 4(b) presents the fracture processes for a model corresponding to the dynamic loading-rate model (within 240μs ~ 345μs). Notably, the incident stress wave have not arrived at the front of the specimen prior to 240μs. At 240 μs, the crack had begin to form in the front of the specimen notch tip. At 270 μs, the several cracks have branched off, with each continuously propagating along a random path. At 285 μs, several cracks are merged and propagated along the loading direction. This process of crack branching, merging, and propagation is continuously repeated until the specimen is entirely divided into two fragments at 345 μs.

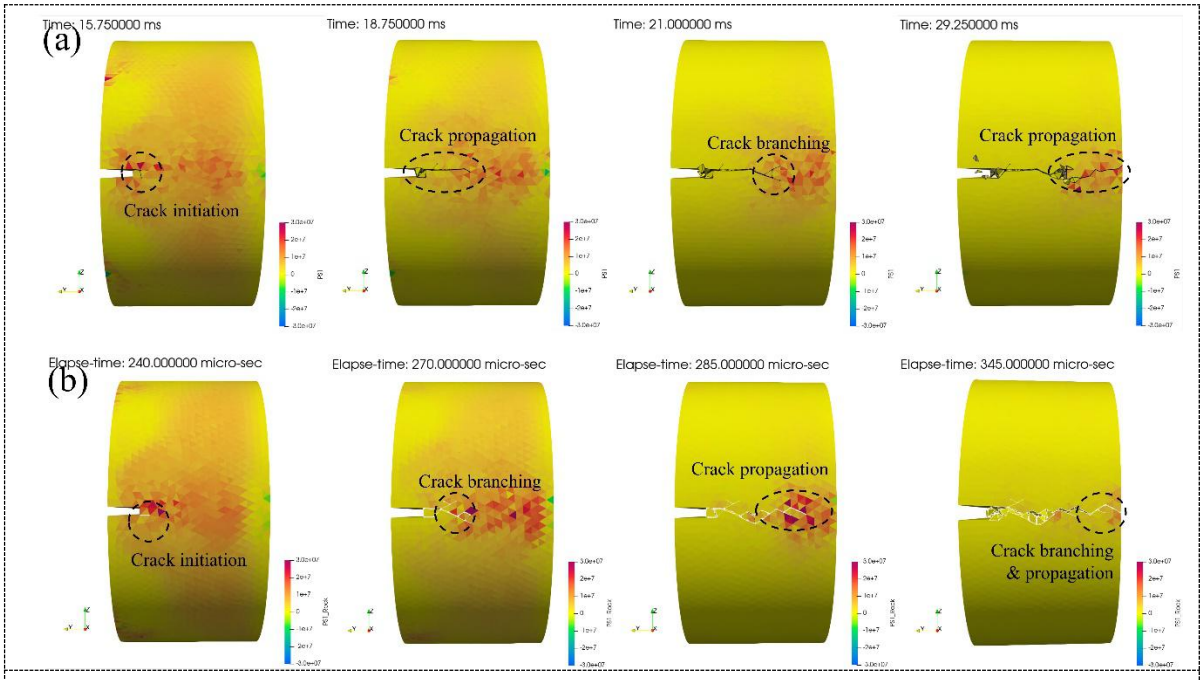

Figure 4. Numerical simulation result of SNDB test under (a) static and (b) dynamic loading

4. Loading-rate dependency on Mode I fracture toughness of anisotropic rock

Fig.5 shows the load and stress profiles under quasi-static and dynamic loading conditions with different orthotropic planes as the fracture plane. Fig.5(a) presents the load-displacement curves resulting from the SNDB test under quasi-static conditions, while Fig.5(b) shows the stress wave profiles from the dynamic SNDB test (transmitted wave) in different orthotropic fracture planes of the

SNDB specimen. Comparing these two figures, it appears that the stiffness between the different orthotropic planes is almost equivalent under quasi-static and dynamic loading conditions, while peak loading is entirely different. In quasi-static loading conditions (Fig.5(a)), the maximum loading value is highest in the Hardway plane, second-highest in the Grain plane, and lowest in the Rift plane. Micro-crack density is most significant in the Rift plane, lower in the Grain plane, and lower still in the Hardway plane. Fig.5(b) highlights that this order is equivalent to the quasi-static loading condition in the case of dynamic loading conditions. The primary difference between these conditions is variation in the maximum loading and stress between orthotropic planes. Under static loading conditions, orthotropy may significantly affect maximum loading, while maximum stress exerts only a minor effect under dynamic loading conditions. The orthotropic effect on Mode I fracture toughness also can be observed in Fig. 6. In Fig. 6, Mode I fracture toughness is observed to increase with the loading-rate increment, even as the orthotropic effect is minimized as the loading-rate is increased. The differences of orthotropic effect on the Mode-I fracture toughness between static and dynamic loading conditions might be from the differences in crack propagation. According to Kipp et al. [14], cracks propagate along with the weakest parts (micro-cracks) and result in a failure surface. Many fine cracks are generated in dynamic loading states where stress has concentrated due to the numerous fracture energies accumulated there. The fracturing tends to ignore the formation of microscopic cracks. Because our simulation also exhibits tensile stress concentration (see Fig. 4), the cracks may be propagated regardless of inherent micro-crack orientation and present a minor orthotropy effect on the Mode I fracture toughness.

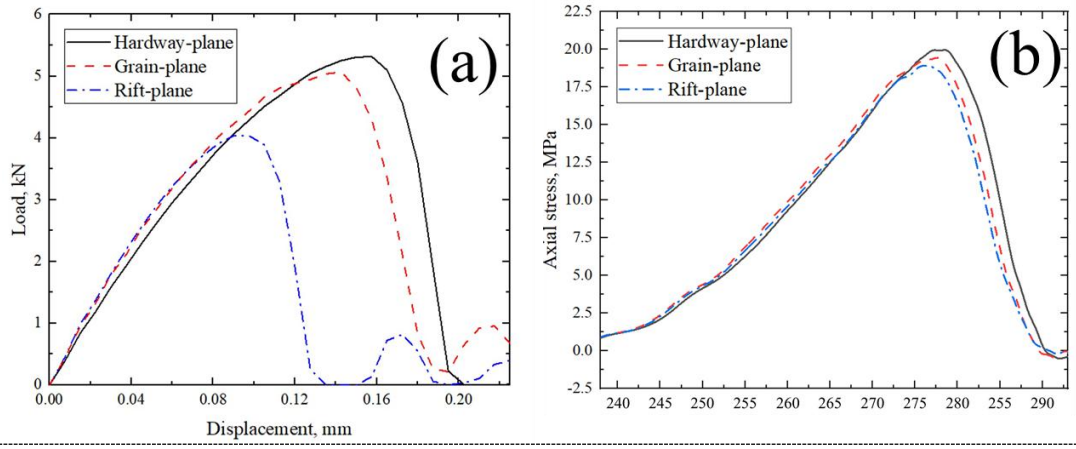

Figure 5. Load and stress profile of (a) the quasi-static SNDB test and (b) the dynamic SNDB test (transmitted wave) under the different orthotropic plane

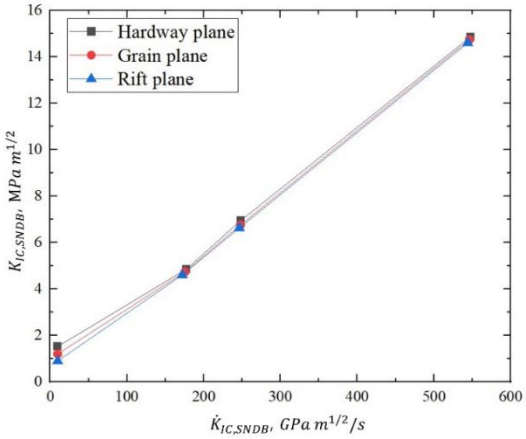

Figure 6. Mode I fracture toughness of anisotropic rock under different loading-rate

5. Conclusion

We have developed a GPGPU based FDEM code to analyze the fracture behavior of an anisotropic rock under different loading-rate conditions. We used an NSCS to determine the anisotropic of granite, in which the orthotropic effective elastic tensor is calculated using only three directions of the P-wave velocity of the rock specimen. The dynamic Mode I fracture toughness using the SNDB specimen (granite), where we assumed an orthotropic elastic body, was then simulated under different loading-rate conditions (i.e., quasi-static and dynamic). The dynamic SNDB simulation results were consistent with those obtained from an experimental dynamic SNDB test. While the GPGPU based FDEM was unable to perform tests in a static condition, the performed quasi-static SNDB test results were consistent with the results of our real-world tests of loading-rate in quasi-static conditions. The SNDB test also presented that the orthotropic characteristic significantly affects the Mode I fracture toughness under quasi-static conditions. However, under dynamic loading conditions, the orthotropic characteristic had minorly affected the Mode I fracture toughness. The fracture pattern also depended on orthotropy in the static or quasi-static condition, while it was almost independent under dynamic loadings.

Acknowledgments

This research was supported by Basic Science Research Program through the National Research Foundation of Korea (NRF) funded by the Ministry of Education (2020R1I1A3074451). The authors would like to thank the Writing Center at Jeonbuk National University for its skilled proofreading service.

References

[1] Birch F 1960 The Velocity of Compressional Waves in Rocks to 10-Kilobars, Part 1 *J Geophys Res* **65** 1083-102
[2] Dai F and Xia K W 2010 Loading Rate Dependence of Tensile Strength Anisotropy of Barre Granite *Pure Appl Geophys* **167** 1419-32
[3] Dai F and Xia K W 2013 Laboratory measurements of the rate dependence of the fracture toughness anisotropy of Barre granite *Int J Rock Mech Min* **60** 57-65
[4] Oh S W, Min G J, Park S W, Kim M S, Obara Y and Cho S H 2019 Anisotropic influence of fracture toughness on loading rate dependency for granitic rocks *Eng Fract Mech* **221** 106677
[5] Oh S-W, Min G-J, Kim M-S, Obara Y, Lee S-E and Cho S-H 2017 Loading Rate Dependency of Fracture Toughness Anisotropy for Granite. In: *4th ISRM Young Scholars Symposium on Rock Mechanics*: International Society for Rock Mechanics and Rock Engineering)
[6] Kataoka M 2015 Fundamental study on fracture toughness and fracture mechanism of rocks. PhD thesis, Kumamoto Univ., Kumamoto)

[7] Sakurada I, Nukushina Y and Ito T 1962 Experimental determination of the elastic modulus of crystalline regions in oriented polymers *Journal of Polymer Science* **57** 651-60
[8] Munjiza A 1992 Discrete elements in transient dynamics of fractured media. Swansea University)
[9] Nara Y and Kaneko K 2006 Sub-critical crack growth in anisotropic rock *Int J Rock Mech Min* **43** 437-53
[10] Tutluoglu L and Keles C 2011 Mode I fracture toughness determination with straight notched disk bending method *Int J Rock Mech Min* **48** 1248-61
[11] Fukuda D, Liu H Y, Zhang Q B, Zhao J, Kodama J, Fujii Y and Chan A H C 2021 Modelling of dynamic rock fracture process using the finite-discrete element method with a novel and efficient contact activation scheme *Int J Rock Mech Min* **138** 104645
[12] Fukuda D, Mohammadnejad M, Liu H Y, Zhang Q B, Zhao J, Dehkhoda S, Chan A, Kodama J and Fujii Y 2020 Development of a 3D Hybrid Finite-Discrete Element Simulator Based on GPGPU-Parallelized Computation for Modelling Rock Fracturing Under Quasi-Static and Dynamic Loading Conditions *Rock Mech Rock Eng* **53** 1079-112
[13] Oh S 2020 Suggestion of Experimental Techniques for Determining the Dynamic Fracture Properties of Rocks. (Republic of Korea: Jeonbuk National University)
[14] Kipp M E, Grady D E and Chen E P 1980 Strain-Rate Dependent Fracture Initiation International Journal of Fracture 16 471-8